Journal of Physics:
Conference Series

PAPER • OPEN ACCESS

Performance analysis of a direct contact humidifier of a humidification-dehumidification desalination system: A heat and mass transfer

To cite this article: M A Galal *et al* 2025 *J. Phys.: Conf. Ser.* **3058** 012014

Journal of Physics: Conference Series **3058** (2025) 012014 doi:10.1088/1742-6596/3058/1/012014

Performance analysis of a direct contact humidifier of a humidification-dehumidification desalination system: A heat and mass transfer

M A Galal[1], R N Abdelmessih[1] and E M Mina[1]

[1] Mechanical Power Engineering, Ain Shams University, Cairo,11517 , Egypt.
E-mail: Mohamed_ashraf@eng.asu.edu.eg

Abstract. In humidification-dehumidification water desalination (HDHWD) systems, the direct contact heat exchanger serves as a crucial component that significantly affects the efficiency of converting saline or brackish water into fresh water. This research focuses on the development of a numerical model to simulate heat and mass transfer processes occurring between hot sprayed seawater and air within a direct-contact humidifier. The model was employed to examine the influence of various operational parameters, including the inlet temperature of seawater, seawater mass flow rate, inlet air temperature, and air mass flow rate, on the humidifier's effectiveness and the rate of freshwater evaporation. The results demonstrate that the optimal humidifier effectiveness is attained when the mass flow rate ratio of seawater to air is unity. Additionally, the inlet temperature of seawater and the mass flow rate ratio between seawater and air emerged as the most critical factors governing the humidifier's freshwater production capacity. The maximum value of water evaporation is 341 kg/hr that occurs at operating conditions of inlet seawater temperature of 90℃, inlet air temperature of 30℃, inlet air relative humidity of 50%, and seawater to air mass ratio of 5. The findings found that freshwater productivity improves by approximately 25% when the seawater temperature is increased by 10%.

1. Introduction

Water is an indispensable resource for all living organisms on Earth, serving as a cornerstone for the survival, development, and reproduction of plants, animals, and humans. However, water scarcity has emerged as a critical global challenge, limiting access to safe and clean drinking water for numerous communities. To address this issue, innovative solutions such as the Humidification-Dehumidification (HDHWD) desalination method offer a sustainable approach to augmenting water supply. This technique enables the efficient utilization of abundant saline water sources, including seawater and brackish water, thereby reducing dependence on traditional freshwater resources. (HDHWD) systems are particularly well-suited for providing freshwater in small-scale, decentralized settings, especially in remote or water-scarce regions where access to potable water is limited. These systems can effectively serve as independent water treatment units, supplying freshwater for drinking purposes and supporting agricultural activities in arid and semi-arid regions. Moreover, their adaptability makes them ideal for off-grid and isolated applications, such as on islands, in coastal areas, or within remote facilities. Many studies have investigated different techniques for (HDHWD) systems. Here are some of the articles that presented research on this type.

Dehghani et al. [1] implemented a mathematical model of a closed air open water (CAOW) HDH desalination system that is coupled with a vapor compression heat pump coupled with a direct contact dehumidifier by using sprayed cold fresh water. Their study evaluated several performance metrics, including recovery ratio, coefficient of performance (COP), and specific electrical energy consumption (SEEC), under varying conditions such as freshwater temperature, saline water temperature, the mass flow rate ratio of saline water to air, and the mass flow rate ratio of saline water to freshwater. The findings show that the working conditions that lead to the highest values of water productivity occur at higher values of (SEEC) as well. In their experimental investigation of the performance of a heat pump-driven HDH desalination system in conjunction with a heat solar collector, Xu et al. [2] discovered that the humidification process is significantly enhanced by the air outlet temperature. The system's total productivity rises when the air temperature rises because the relative humidity falls, enabling more water to evaporate. The study that presented by Ge et al. [3] showed how regulating the temperature of the air outlet might improve the humidification process, especially by keeping the temperature at a level that maximizes the uptake of water vapor without using too much energy. A comprehensive discussion of the HDH desalination method was presented by Rahimi-Ahar et al. [4], who emphasized that elements like surface area, air-water interaction time, and the temperature difference between the water and air all affect how effective the humidifier is. Lawal et al. [5] discussed various strategies to enhance the effectiveness of humidifiers, such as optimizing the design of the packing material inside the humidifier, which increases the surface area for air-water contact and improves the freshwater productivity. The performance analysis of a two-stage indirect solar dryer in conjunction with an HDH desalination system was studied by Kabeel et al. [6]. They discovered that the system's total water production rate was improved by the evaporation rate, which rose noticeably with higher air temperatures and lower air humidity. Hussain Soomro et al. [7] investigated how humidifier parameters affected a small-scale HDH desalination system's efficiency and showed that adjusting the air and water flow rates may greatly boost the evaporation rate, increasing the desalination process' efficacy. Qundong Zhu et al. [8] investigated the heat and mass transfer characteristics of humidifiers in Humidification-Dehumidification (HDH) desalination systems. A heat-mass coupled differential equation model was developed to analyze the effects of various parameters, such as spray water temperature, mass flow rate of spray water, air temperature, and air mass flow rate, on the humidification performance of eight different packing materials. The results indicate that cellulose paper exhibits the best humidification performance, followed by polypropylene and hackettes. Increasing seawater temperature significantly enhances humidification performance, with optimal performance achieved at temperatures above 80 °C. The study provides theoretical guidance for selecting efficient packing materials. Zhang et al. [9] conducted a numerical and experimental investigation for the performance of HDH system coupled with heat pump system. The results showed that, as the airflow rate increases, unit productivity gradually rises until reaching a maximum value, after which it declines with further increases in airflow. In contrast, an increase in seawater flow rate consistently enhances freshwater yield. Zhani et al. [10] presented a validation of a transient numerical model for air and water flat-plate solar collectors used for HDH solar desalination systems with experimental work. They noticed that the experimental and numerical water temperature results share similar patterns with a small error due to the position of the sensors, which are in contact with the outer surface of the pipe instead of inside it. He et al. [11] investigated the performance of a humidification–dehumidification desalination system integrated with a vapor compression heat pump. Heat rejected from the condenser of the heat pump was utilized to elevate the temperature of feed saline water to the top system temperature, while the rejected brine was employed to evaporate the refrigerant in the evaporator of the heat pump. Maximum freshwater of 82.12 kg/hr and 106.53 kg/hr were obtained at the system pressure ratio (PR) of 4 and 5 respectively. The highest recorded GOR of the system was found to be 5.14, which was attained at PR of 4. Lawal et al.[12] experimentally assessed the performance of a horizontal crossflow packed-bed HDH configuration with mass balancing. The system is a closed water (brine recirculation), open-air configuration. Mass extraction and injection are reported to enhance system performance. About 1.33%, 6.02 L/hr, and 2.7 were reported as the peak system recovery ratio, freshwater productivity and gained output ratio, respectively. Kaunga et al. [13] developed a model by integrating the heat and mass transfer equations at the Liquid–gas interface into enthalpy-based equations. The performance of the proposed model is evaluated by comparing it with an empirical model from the literature, using experimental data obtained from the HDH system designed in this study. The findings reveal that the system's recovery ratio increases significantly with rising feed water temperature but decreases as the seawater to air flow ratio increases. Freshwater productivity improves with an increase in the packing's specific area, while doubling the dehumidifiers' surface area enhances the recovery ratio by 16%. Khan et al. [14] carried out experiments to compare single and double stage air heated HDH desalination systems. The results showed that the double stage system performs higher values in water productivity and gain output ratio (GOR) than single stage HDH system.

Therefore, based on the reviewed literature on HDH desalination systems, the impacts of mass flow rate of air and seawater on humidifier effectiveness have not been addressed in previous research. This study investigates these effects to optimize humidifier effectiveness. In the present work, we utilize a differential equation mathematical model to explore the control volume of the researched element of the direct contact humidifier through structured packing, hence optimizing the humidifier's performance by studying the impact of inlet seawater temperature, seawater mass flow rate, inlet air temperature and air mass flow rate on humidifier effectiveness and freshwater evaporation rate. After that, determine the optimum operating conditions to attain the highest output values.

NOMENCLATURE

a_p	Specific surface area of the packing $\left(\frac{m^2}{m^3}\right)$
A_c	Cross-section area of the packing (m^2)
c_p	Specific heat $(\frac{\mathrm{J}}{\mathrm{kg.K}})$
α	Heat transfer coefficient $(\frac{\mathrm{W}}{m^2.\mathrm{K}})$
$\dot{m}_{ev}$	Total freshwater evaporation rate $(\frac{kg}{hr})$
$\dot{m}$	Mass flow rate $(\frac{kg}{s})$
dz	Step of the studied element height (m)
h_{fg}	Latent heat of vaporization $(\frac{\mathrm{J}}{kg})$
β	Mass transfer coefficient $(\frac{m}{\mathrm{s}})$
MR	Seawater to air mass flow rate ratio
T	Temperature (°C)
H	Enthalpy $(\frac{\mathrm{J}}{s})$

Greek Letters

ω	Humidity ratio $(\frac{kg_{wv}}{kg_{da}})$
ρ	Density $(\frac{kg}{m^3})$
ϕ	Relative humidity (%)
ε	Humidifier effectiveness

Subscripts

a	Dry air
int	Interface
p	Packing
sw	Seawater
ev	Evaporation

2. Model Description

Figure 1. shows the overview of the direct contact humidifier of an (HDHWD) cycle. As shown, the direct contact heat exchanger consists of nozzles that are used to achieve a spray zone of seawater that sprayed over a packing bed to provide a large surface area for seawater-air interaction. The type of packing which is used in this study is polypropylene material, which has a higher specific surface area of $a_p = 350\ \left(\frac{m^2}{m^3}\right)$, and cross-sectional area of $A_c = 0.1\ m^2$ with height of 0.6 m.

In HDHWD cycle, the hot saline water is sprayed over the packing bed through nozzles meeting the inlet air in counter direction. As the air passes over the wetted surfaces, it absorbs water vapor, increasing its humidity. As heat is supplied to the interface between air and water, it provides the latent heat needed to cause water molecules to leave the interface to the air stream, effectively separating the water from the dissolved salts.

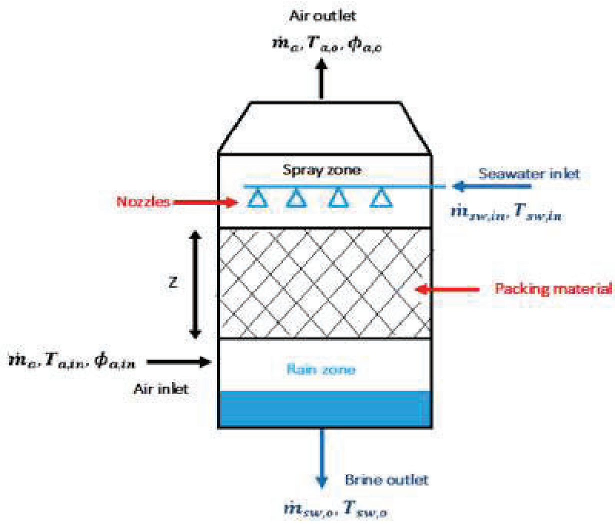

Figure 1. Schematic of the packed-bed direct-contact humidifier of a HDHWD cycle.

Based on heat and mass transfer relations between air and sprayed seawater in a control volume of packing height which expressed in Figure 2. The heat and mass transfer between an interface layer on the surface of the water and the bulk air controls the outputs of the computational element.

This model is solved based on the following assumptions:

- When the spray water and air inside the humidifier were thermally exchanging, the heat transfer between the humidifier and the surrounding air was ignored.
- The seawater temperature must not be less than the inlet temperature of air.
- Mass transfer and heat transfer areas were equivalent.
- The heat and mass transfer process within the humidifier remains in a steady state.

The sensible heat extracted from the water element in terms of the energy balance on the water side is expressed in the form of:

$$\dot{Q}_{sensible,water} = \dot{m}_{sw}\, c_w\, dT_{sw} \tag{1}$$

The rate of heat transfer between the water and the interface is expressed in the form of:

$$\dot{Q}_{sensible,water} = h_w\, A_C\, a_p\, dz\ (T_{sw} - T_{int}) \tag{2}$$

where $\dot{m}_{sw}$is the seawater mass flow rate, c_w is the seawater specific heat, h_w is the convection coefficient in the side of the water, A_C is the packing cross-sectional area, a_p is the packing material specific surface area, dz is the studied element height, dT_{sw} is the temperature difference between the inlet seawater to the studied element, and the outlet seawater from the studied element, and T_{int} is the temperature of the interface.

The sensible heat added to the air element in terms of the energy balance on the air side is expressed in the form of:

$$\dot{Q}_{sensible,air} = \dot{m}_a\, c_a\, dT_a \tag{3}$$

The rate of heat transfer between the air and the interface is expressed in the form of:

$$\dot{Q}_{sensible,air} = h_a\, A_C\, a_p\, dz\ (T_{int} - T_a) \tag{4}$$

where $\dot{m}_a$ is the air mass flow rate, c_a is the air specific heat, h_a is the convection coefficient in the side of the air, dT_a is the temperature difference between the inlet air to the studied element and the outlet air temperature from the studied element which expected to increase on moving up the packing.

The mass transfer of fresh water that transferred to the air is expressed in the form:

$$\dot{m}_{ev} = h_m\, A_C\, a_p\, dz\ (\omega_{int} - \omega_a) \tag{5}$$

The rate of freshwater evaporated in the air in terms of mass balance between inlet and outlet element is calculated from the equation:

$$\dot{m}_{ev} = \dot{m}_a\, d\omega_a \tag{6}$$

The latent heat that added to the air is expressed in the form:

$$\dot{Q}_{latent} = \dot{m}_{ev}\ h_{fg} \tag{7}$$

where m_{ev} is the mass flow rate of evaporated water in air, ω_{int} is the interface humidity ratio, ω_a is the humidity ratio of air through the humidifier, h_{fg} is latent heat of vaporization and h_m is the mass transfer coefficient.

By applying energy balance between air and water:

$$\dot{Q}_{sensible,air} + \dot{Q}_{latent} = \dot{Q}_{sensible,water} \tag{8}$$

We get the values of dT_a(i), dT_{sw}(i), $d\omega_a$(i), and $d\dot{m}_{ev}$(i) by solving the previous equations simultaneously. These values are used to obtain the values of next step using Euler method.

For the upcoming steps, the following equations are used to express the change in each step by solving each element step using Newton Rapson method.

$$T_a(\text{i+1}) = T_a(\text{i}) + dT_a(\text{i}) \tag{9}$$

$$T_{sw}(\text{i+1}) = T_{sw}(\text{i}) + dT_{sw}(\text{i}) \tag{10}$$

$$\omega_a(\text{i+1}) = \omega_a(\text{i}) + d\omega_a(\text{i}) \tag{11}$$

This model is valid to be applied to any assumption of inlet parameters for air and water inlet conditions. In reality, variations in these parameters can significantly influence the performance of the direct-contact humidifier, which will be discussed in the following results section. In addition, the model can be used successfully for a different humidifier geometry and different types of packing material properties.

The system performance is assessed using a variety of non-dimensional characteristics under different operating conditions. In the humidifier, the mass flow rate ratio of seawater to air is crucial to the device's performance.

$$MR = \frac{\dot{m}_{sw}}{\dot{m}_a} \tag{12}$$

In the humidifier, the effectiveness of the component is defined as a comparison of the actual thermal energy against ideal thermal energy transferred from each stream and is expressed as the change of actual enthalpy rate to the maximum possible change in enthalpy rate [1]. Therefore, the humidifier's effectiveness would be denoted as follows:

$$\varepsilon = max\left(\frac{H_{a,o} - H_{a,in}}{\dot{H}_{a,o}^{\ ideal} - H_{a,in}}, \frac{H_{sw,in} - H_{sw,o}}{H_{sw,in} - \dot{H}_{sw,o}^{\ ideal}}\right) \tag{13}$$

In the humidifier, the ideal enthalpy of outlet air ($\dot{H}_{a,o}^{\ ideal}$) occurs when the exit air from the humidifier is totally saturated at the seawater inlet temperature and the ideal enthalpy of seawater ($\dot{H}_{sw,o}^{\ ideal}$) happens when its temperature is equal to the inlet air temperature.

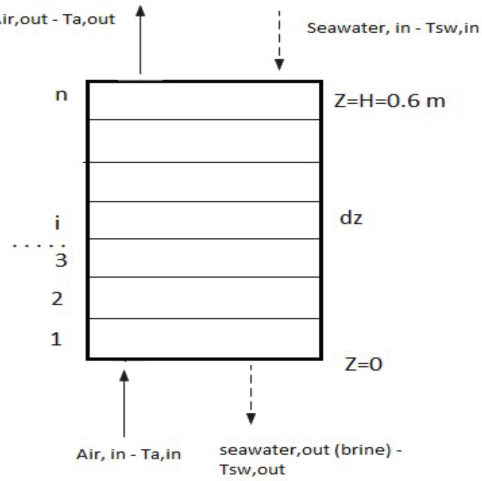

Figure 2. Schematic diagram of the humidifier control volume.

3. Validation of the model

The mathematical model developed in this research is validated by comparing it with the humidifier study that was experimentally studied by Zhang et al. [9] and the numerical model that was developed by Qundong Zhu et al. [8], which was presented in Figure 3. The humidifier packing properties that are utilized in Zhang et al. [9] and Qundong Zhu et al. [8] models are based on polypropylene material type, (500 mm x 500 mm) cross-sectional area with 2.5 m height. It is observed that under the same operation conditions ($\dot{m}_a = 1\ kg/s$, T_{sw}= 50℃, T_a= 16℃, $\phi_{a,in} = 10\ \%$), the average error is 2% from the experimental results, which is an acceptable error. The system's pertinent operational parameters were adjusted to examine the humidifier performance.

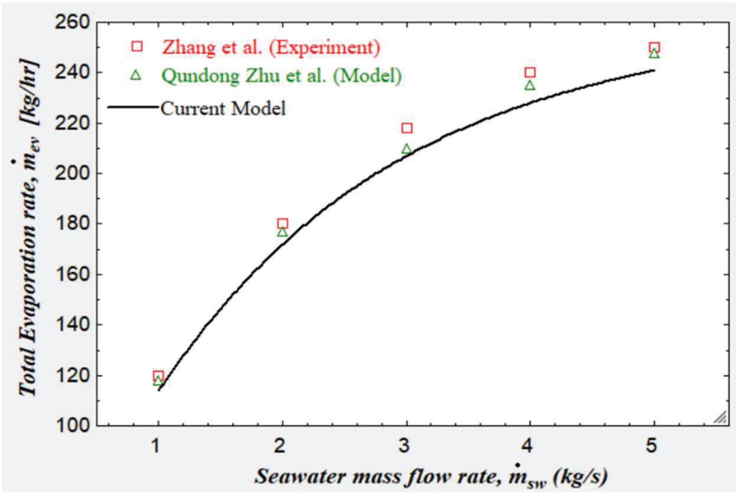

Figure 3. Comparison of the total freshwater evaporation rate between the numerical model in this paper, Zhang et al. [9] (experiment data) and Qundong Zhu et al. model [8]

4. Results and Discussion

4.1. Effect of air mass flow rate on humidifier effectiveness and freshwater evaporation rate.

Figure 4. illustrates how variations in air mass flow rate affect humidifier effectiveness at various seawater mass flow rate values. It demonstrates that, as the input air mass flow rate rises, effectiveness may first decline to a certain value before increasing.

At lower values of the air mass flow rates, there is a significant ratio of saltwater to air mass flow rate. This shows that the air has adequate time to absorb humidity from the saltwater as it flows inside the humidifier and that there is a substantial amount of seawater with relation to the air. Due to the air's restricted capacity to collect both moisture and heat in contrast to the saltwater that is easily available, air side efficacy is the limiting factor. So, since the air side heat and mass transfer rate drop with an increase in the air mass flow rate, the humidifier's effectiveness drops dramatically.

As the air mass flow rate increases, the saltwater-to-air mass ratio decreases and the air in this region begins to absorb heat and moisture from the seawater more effectively. However, any curve in this region is only somewhat beneficial. This happens as a result of an uneven distribution of mass and heat between the air and water sides. This lowest point is more obvious at higher seawater flow rates $\dot{m}_{sw} = 2\ kg/s$) due to the greater disparity in mass and heat transfer capacities.

The ratio of saltwater to air mass decreases as air mass flow rates increase. Seawater-side efficacy is currently the main limiting factor because of the seawater's limited capacity to provide heat and moisture compared to the air's capacity to absorb it. The effectiveness of the humidifier increases with air mass flow rate because the available saltwater has been utilized more effectively in this location. The rise is more noticeable at lower seawater flow rates ($\dot{m}_{sw} = 1\ kg/s$) because the air's absorption capacity rises significantly while saltwater remains constant. As shown, when ($MR = 1$), the maximum effectiveness is attained.

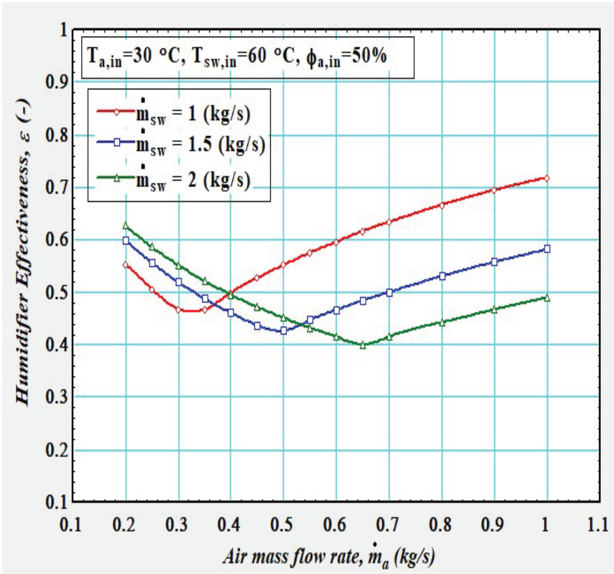

Figure 4. Variation of air mass flow rate with humidifier effectiveness at different values of seawater mass flow rate.

The impact of air mass flow rate variation on the overall freshwater evaporation rate at various seawater mass flow rate values is shown in Figure 5. This means that higher air flow rates will result in an increase in the overall evaporation rate because more air passes through the humidifier, even though each unit of air absorbs slightly less moisture. The freshwater evaporation rate rises by 34% at $\dot{m}_a = 1\ kg/s$ and by 14% at $\dot{m}_a = 0.2\ kg/s$, according to the graph, when the saltwater mass flow rate is doubled. As a result, freshwater productivity varies very little when water flow rates are increased at reduced air flow rates since the air side's capacity to absorb this energy is not much impacted.

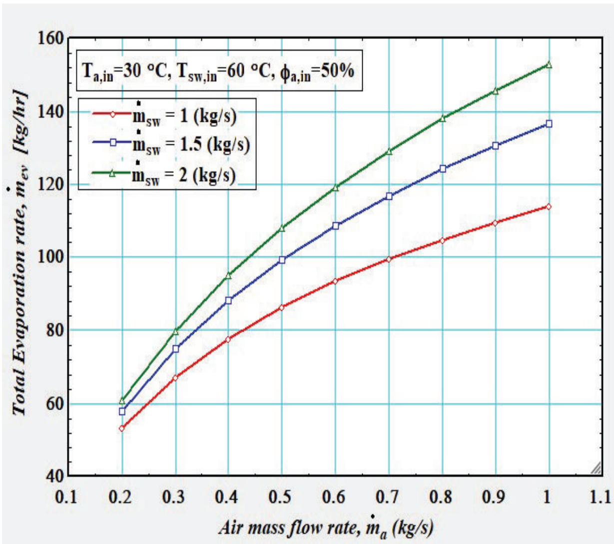

Figure 5. Variation of air mass flow rate with total freshwater evaporation rate at different values of seawater mass flow rate

4.2. Effect of seawater mass flow rate on humidifier effectiveness and freshwater evaporation rate.

Figure 6. displays the impact of the seawater mass flow rate variation on the humidifier effectiveness at different values of air mass flow rate. The effectiveness of a humidifier can exhibit a decrease followed by an increase as the seawater mass flow rate increases. The trend in this graph has the same behavior and explanation as Figure 4.

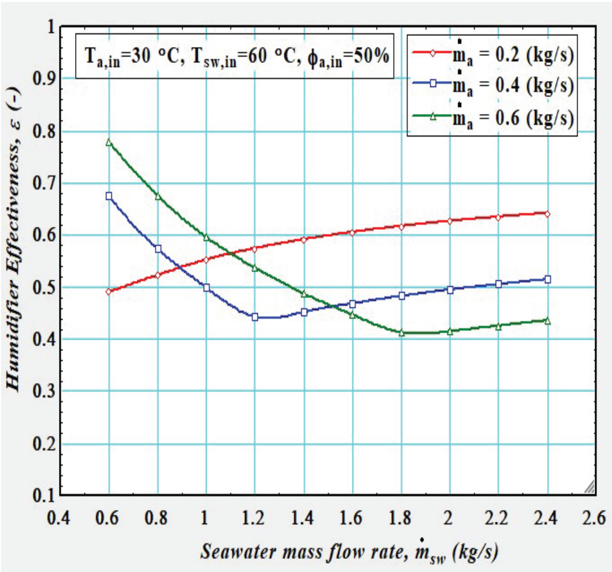

Figure 6. Variation of seawater mass flow rate with humidifier effectiveness at different values of air mass flow rate.

Figure 7. shows that the impact of the seawater mass flow rate variation on the total freshwater evaporation rate at different values of air mass flow rate which shows that a higher values of seawater flow rate can lead to an increased evaporation rate as more water is available to be evaporated into the air.

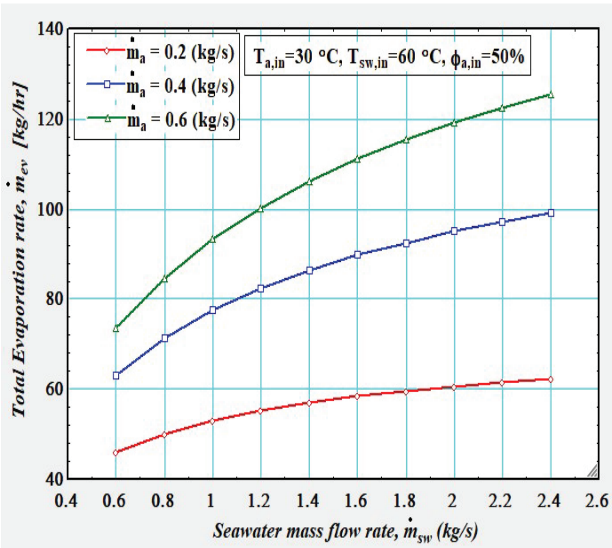

Figure 7. Variation of seawater mass flow rate with total freshwater evaporation rate at different values of air mass flow rate.

4.3. Effect of inlet seawater temperature on freshwater evaporation rate.

Figure 8. illustrates the impact of change the inlet seawater temperature on the total freshwater evaporation rate at different values of seawater to air mass flow rate ratio. By increasing the inlet seawater temperature, the evaporation rate increases significantly because warmer water evaporates more readily.

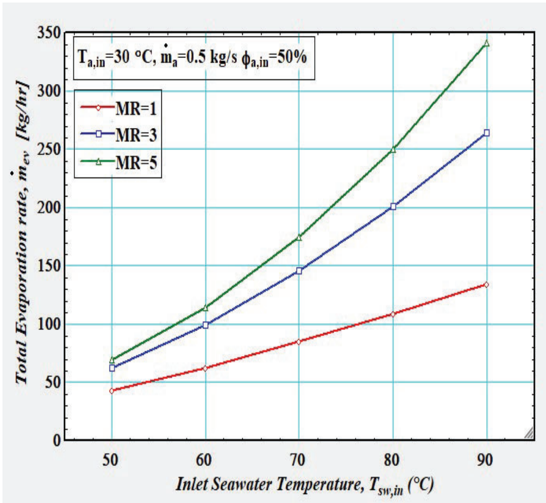

Figure 8. Variation of inlet seawater temperature on total freshwater evaporation rate at different values of seawater to air mass flow rate ratio.

4.4. Effect of inlet air temperature on freshwater evaporation rate.

Figure 9. depicts the influence of the input air temperature change on the total freshwater evaporation rate for various values of saltwater to air mass flow rate ratio. When the air temperature is raised, these gradients diminish if the water temperature stays constant. A lower temperature differential minimizes the heat transfer from the water to the air, which is the principal cause of evaporation. With less heat being transported from the water to the air, the rate at which water molecules gather enough energy to evaporate is lowered.

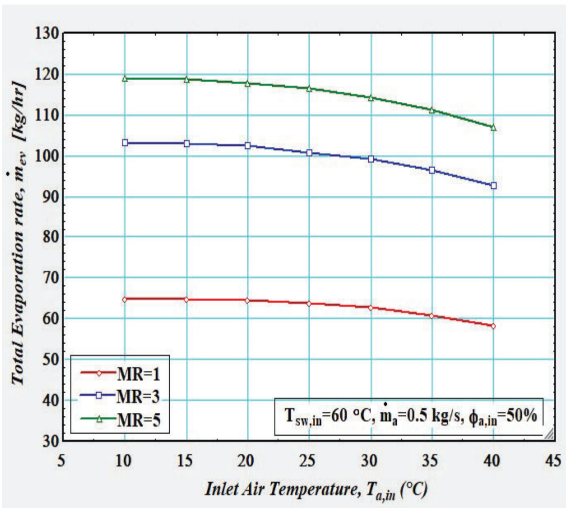

Figure 9. Variation of inlet air temperature on total freshwater evaporation rate at different values of seawater to air mass flow rate.

4.5. Sensitivity analysis

A Sensitivity analysis was developed to determine the influence of key input parameters, including air mass flow rate, water mass flow rate, air inlet temperature, and water inlet temperature, on the freshwater evaporation rate. This analysis is critical for understanding parameter significance and optimizing the design of the HDH desalination system. The analysis was conducted by varying each input parameter individually by ±10% around its baseline value while keeping all other parameters constant.

The baseline values were based on the inlet operating conditions: $T_{sw,in}$=60°C, $T_{a,in}$=30°C, $\dot{m}_a = 0.5\ kg/s$, $\dot{m}_{sw} = 1\ kg/s, and\ \phi_{a,in} = 50\%$. Sensitivity index were calculated for each input parameter using:

$$Sensitivity\ Index\ (S) = \frac{Percentage\ change\ in\ output}{Percentage\ change\ in\ input}$$

The results found that the inlet seawater temperature had the highest influence on the freshwater evaporation rate ($S_{T_{sw}}$= 2.47) while the air inlet temperature had the minimum impact on freshwater evaporation rate (S_{T_a}= -0.163). The air and seawater mass flow rate had a moderate influence on freshwater evaporation rate ($S_{\dot{m}_{a,in}}$=0.418, $S_{\dot{m}_{sw,in}}$= 0.355).

The high sensitivity of the freshwater evaporation rate to seawater temperature rate suggests that precise control of seawater temperature is essential for achieving optimal desalination performance.

5. Conclusion

Mathematical modelling is used to examine the performance analysis of the direct contact humidifier. We may thus conclude that when the system operates in a way that results in a greater rate of water evaporation and humidifier effectiveness.

- Increases in the ratio of seawater to air mass flow rate result in maximum values of freshwater evaporation values.
- The optimum value of humidifier effectiveness is achieved on a unity mass flow rate ratio ($MR = 1$).
- Seawater inlet temperature and mass flow rate ratio are the most critical parameters influencing freshwater production rate.
- The low sensitivity of evaporation rate to air temperature suggests opportunities for energy savings by optimizing air heater operation.
- Freshwater productivity improves by approximately 25% when the seawater temperature increases by 10%.
- The maximum value of water evaporation is 341 kg/hr. that occurs at operating conditions of $T_{sw,in}$=90°C, $T_{a,in}$=30°C, $MR = 5, and\ \phi_{a,in} = 50\%$.

References

[1] Dehghani S, Date A and Akbarzadeh A 2018 Performance analysis of a heat pump driven humidification-dehumidification desalination system *Desalination* **445** 95–104
[2] Xu H, Zhao Y and Dai Y J 2019 Experimental study on a solar assisted heat pump desalination unit with internal heat recovery based on humidification-dehumidification process *Desalination* **452** 247–57
[3] Ge H, Cai Y, Kang P, Liu J and Liu X 2022 Experimental Study on Humidifier Performance in a Humidification-Dehumidification System *Journal of Physics: Conference Series* vol 2186 (IOP Publishing Ltd)
[4] Rahimi-Ahar Z, Hatamipour M S and Ahar L R 2020 Air humidification-dehumidification process for desalination: A review *Prog Energy Combust Sci* **80** 100850
[5] Lawal D U and Qasem N A A 2020 Humidification-dehumidification desalination systems driven by thermal-based renewable and low-grade energy sources: A critical review

Renewable and Sustainable Energy Reviews **125** 109817

[6] Kabeel A E and Abdelgaied M 2018 Experimental evaluation of a two-stage indirect solar dryer with reheating coupled with HDH desalination system for remote areas *Desalination* **425** 22–9

[7] Hussain Soomro S, Santosh R, Bak C U, Yoo C H, Kim W S and Kim Y D 2022 Effect of humidifier characteristics on performance of a small-scale humidification-dehumidification desalination system *Appl Therm Eng* **210** 118400

[8] Zhu Q, Wu W, Ren Y, Wang F and Han Y 2023 Study on the Heat and Mass Transfer Characteristics of Humidifiers in Humidification–Dehumidification Desalination Systems *Energies (Basel)* **16**

[9] Zhang Y, Zhang H, Zheng W, You S and Wang Y 2019 Numerical investigation of a humidification-dehumidification desalination system driven by heat pump *Energy Convers Manag* **180** 641–53

[10] Zhani K, Ben Bacha H and Damak T 2011 Modeling and experimental validation of a humidification-dehumidification desalination unit solar part *Energy* **36** 3159–69

[11] He W F, Han D and Ji C 2018 Investigation on humidification dehumidification desalination system coupled with heat pump *Desalination* **436** 152–60

[12] Lawal D U, Antar M A, Aburub A and Aliyu M 2018 Performance assessment of a cross-flow packed-bed humidification– dehumidification (HDH) desalination system – the effect of mass extraction *Desalination Water Treat* **104** 28–37

[13] Kaunga D, Patel R and Mujtaba I M 2022 Humidification-dehumidification desalination process: Performance evaluation and improvement through experimental and numerical methods *Thermal Science and Engineering Progress* **27**

[14] Khan M, Antar M A, Khalifa A E and Zubair S M 2021 Experimental investigation of air heated bubble column humidification dehumidification desalination system *Int J Energy Res* **45** 2610–28